THE JOURNAL OF BIOLOGICAL CHEMISTRY VOL. 286, NO. 40, pp. 35236–35246, October 7, 2011

Substrate tRNA Recognition Mechanism of a Multisite-specific tRNA Methyltransferase, *Aquifex aeolicus* Trm1, Based on the X-ray Crystal Structure*[S]

Received for publication, April 21, 2011, and in revised form, June 26, 2011 Published, JBC Papers in Press, August 15, 2011, DOI 10.1074/jbc.M111.253641

Takako Awai[‡], Anna Ochi[‡], Ihsanawati[§1], Toru Sengoku[§], Akira Hirata[‡], Yoshitaka Bessho[§¶], Shigeyuki Yokoyama[§¶‖], and Hiroyuki Hori[‡§2]**

*From the [‡]Department of Materials Science and Biotechnology, Graduate School of Science and Engineering, Ehime University, Bunkyo 3, Matsuyama, Ehime 790-8577, the [§]Systems and Structural Biology Center, Yokohama Institute, RIKEN, Suehiro-cho 1-7-22, Tsurumi-ku, Yokohama, Kanagawa 230-0045, the [¶]RIKEN SPring-8 Center, Harima Institute, Kouto 1-1-1, Sayo, Hyogo 679-5148, the [‖]Department of Biophysics and Biochemistry, Graduate School of Science, University of Tokyo, Hongo 7-3-1, Bunkyo-ku, Tokyo 113-0033, and the **Venture Business Laboratory, Ehime University, Bunkyo 3, Matsuyama, Ehime 790-8577, Japan*

Archaeal and eukaryotic tRNA (N^2,N^2-guanine)-dimethyltransferase (Trm1) produces N^2,N^2-dimethylguanine at position 26 in tRNA. In contrast, Trm1 from *Aquifex aeolicus*, a hyper-thermophilic eubacterium, modifies G27 as well as G26. Here, a gel mobility shift assay revealed that the T-arm in tRNA is the binding site of *A. aeolicus* Trm1. To address the multisite specificity, we performed an x-ray crystal structure study. The overall structure of *A. aeolicus* Trm1 is similar to that of archaeal Trm1, although there is a zinc-cysteine cluster in the C-terminal domain of *A. aeolicus* Trm1. The N-terminal domain is a typical catalytic domain of *S*-adenosyl-L-methionine-dependent methyltransferases. On the basis of the crystal structure and amino acid sequence alignment, we prepared 30 mutant Trm1 proteins. These mutant proteins clarified residues important for *S*-adenosyl-L-methionine binding and enabled us to propose a hypothetical reaction mechanism. Furthermore, the tRNA-binding site was also elucidated by methyl transfer assay and gel mobility shift assay. The electrostatic potential surface models of *A. aeolicus* and archaeal Trm1 proteins demonstrated that the distribution of positive charges differs between the two proteins. We constructed a tRNA-docking model, in which the T-arm structure was placed onto the large area of positive charge, which is the expected tRNA-binding site, of *A. aeolicus* Trm1. In this model, the target G26 base can be placed near the catalytic pocket; however, the nucleotide at position 27 gains closer access to the pocket. Thus, this docking model introduces a rational explanation of the multisite specificity of *A. aeolicus* Trm1.

Methylation is one of the most common chemical modifications that occurs in a broad range of biomolecules, including nucleic acids, proteins, lipids, and small compounds. It is implicated in a variety of cellular processes, such as translation, transcription, processing of RNA, epigenetics, development, carcinogenesis, neurotransmission, cellular transport, infection, and bacterial host defense. Among the RNA species, methylated nucleotides appear in most noncoding RNAs, constituting more than half of the post-transcriptional modifications identified so far. In particular, tRNA contains abundant methylated nucleotides, which stabilize the L-shaped tRNA structure and improve their molecular recognition (1–3).

Among the methylated nucleotides in tRNA, N^2,N^2-dimethylguanine at position 26 (m^2_2G26) is a common modification and is generated by tRNA (N^2,N^2-guanine)-dimethyltransferase (tRNA (m^2_2G26) methyltransferase (m2, 2G26); EC 2.1.1.32) (Fig. 1, *A* and *B*) (2, 3). This enzyme catalyzes the methyl transfer reaction from *S*-adenosyl-L-methionine (AdoMet)[3] to the N^2 atom of G26, which is located at the junction between the D-arm and the anticodon-arm in tRNA. In the reaction, two molecules of AdoMet are consumed, and N^2-methylguanine at position 26 (m^2G26) is generated as an intermediate (4). Thus, in some cases, this enzyme catalyzes the transfer of only one methyl group and functions as a tRNA (m^2G26) methyltransferase (5). The enzymatic activity was initially detected in rat liver (6, 7) and subsequently found in various organisms (8–12). The most highly purified enzyme from a native source was obtained from *Tetrahymena pyriformis* (4). The responsible gene was first determined to be *trm1* from *Saccharomyces cerevisiae* (13, 14) and then experimentally identified from various eukaryotes (*Schizosaccharomyces pombe* (15), *Caenorhabditis elegans* (16), and human (17)) and archaea (*Pyrococcus furiosus* (18), *Pyrococcus horikoshii* (19), and *Haloferax volcanii* (20)), consistent with the distribution of the m^2_2G26 (or m^2G26) modification in tRNA. Furthermore, we have recently reported that *Aquifex aeolicus*, a hyper-thermophilic eubacterium, has a Trm1 protein that catalyzes methyl transfer not only to G26 but also to G27 (21).

* This work was supported in part by Grant-in-aid for Science Research on Priority Areas 20034041 (to H. H.), Grants-in-aid for Science Research 19350087 and 2350081 (to H. H.) and 21603018 (to Y. B.), and the National Project on Targeted Proteins Research Program for Science Research from the Ministry of Education, Science, Sports, and Culture of Japan.

[S] The on-line version of this article (available at http://www.jbc.org) contains supplemental Table 1 and Figs. 1 and 2.

The atomic coordinates and structure factors (codes 3AXT and 3AXS) have been deposited in the Protein Data Bank, Research Collaboratory for Structural Bioinformatics, Rutgers University, New Brunswick, NJ (http://www.rcsb.org/).

[1] Present address: Biochemistry Research Group, Institut Teknologi Bandung, Ganesa 10, Bandung, West Java 40132, Indonesia.

[2] To whom correspondence should be addressed. Tel.: 81-89-927-8548; Fax: 81-89-927-9941; E-mail: hori@eng.ehime-u.ac.jp.

[3] The abbreviation used is: AdoMet, *S*-adenosyl-L-methionine.

In general, methylated nucleotides in tRNA are post-transcriptionally produced by site-specific methyltransferases (3). However, there are some cases in which one tRNA methyltransferase modifies multiple sites in substrate tRNA. Thus, some tRNA methyltransferases have a multisite specificity. For example, *Pyrococcus abyssi* TrmI catalyzes methyl transfer to both A57 and A58, forming m^1A57 and m^1A58, respectively (22). In addition, eukaryotic Trm4 is responsible for 5-methylcytidine formation at positions 34, 40, 48, and 49 in tRNA (23). Furthermore, it has been reported that *P. abyssi* PAB1947 protein (archaeal Trm4) changes its site specificity in the presence of PAB1946 protein (archaese) (24). Moreover, *S. cerevisiae* Trm7 protein catalyzes 2′-*O*-methylation of nucleotides at positions 32 and 34 (25). As described above, we previously reported that *A. aeolicus* Trm1 has a multisite specificity (21). Although these examples have been reported, there is little knowledge concerning the mechanism of multisite recognition. In this study, we focus on the multisite specificity of *A. aeolicus* Trm1.

EXPERIMENTAL PROCEDURES

Materials—[*methyl*-^{14}C]AdoMet (1.95 GBq/mmol) and [*methyl*-^{3}H]AdoMet (2.47 TBq/mmol) were purchased from ICN. Cold AdoMet was obtained from Sigma. DE52 is a product of Whatman. CM-Toyopearl 650 M was from Tosoh. DNA oligomers were bought from Invitrogen, and T7 RNA polymerase was from Toyobo. Other chemical reagents were of analytical grade.

Preparation of Recombinant A. aeolicus Trm1—The recombinant *A. aeolicus* Trm1 was purified according to our previous report (21). Site-directed mutagenesis was performed by a QuikChange® mutagenesis kit (Stratagene).

Measurement of Enzymatic Activity and Kinetic Parameters—The standard assay used during the purification process measured the incorporation of ^{14}C-methyl groups from [*methyl*-^{14}C]AdoMet into the *A. aeolicus* tRNA^{His} transcript by incubating 0.1 μM enzyme, 11 μM transcript, and 38 μM [*methyl*-^{14}C]AdoMet in 45 μl of buffer A (50 mM Tris-HCl, pH 7.5, 5 mM $MgCl_2$, 6 mM 2-mercaptoethanol, and 50 mM KCl) for 15 min at 55 °C. An aliquot (30 μl) was then used for the filter assay. RNA transcripts were prepared as reported previously (26). If discrimination between the m^2G and $m^2{}_2$G formation activities was necessary, we employed two-dimensional thin layer chromatography as described in our previous reports (21, 27). Prior to measuring the kinetic parameters, we performed time course experiments at 55 °C with 0.1 μM Trm1, 11 μM yeast tRNA^{Phe} transcript, and 38 μM [*methyl*-^{14}C]AdoMet in 210 μl of buffer A. Because the three-dimensional structure of yeast tRNA^{Phe} has been well studied and this tRNA has a G26C27 sequence (28, 29), we used the yeast tRNA^{Phe} transcript as substrate. Aliquots (30 μl each) were taken at appropriate times (0, 2, 5, 7.5, 10, and 15 min), and the formations of ^{14}C-pm^{2}G and ^{14}C-pm$^2{}_2$G were monitored by two-dimensional TLC. Under these conditions, only pm^{2}G increased linearly for the first 10 min, and $m^2{}_2$G formation was barely observable; the pm$^2{}_2$G content was less than 5% of the pm^{2}G content in the sample at 10 min. After this pilot experiment, we determined the kinetic parameters of the first methylation (m^2G26 formation). For measurements of kinetic parameters for AdoMet, 0.1 μM Trm1, 11 μM tRNA^{Phe} transcript, and various concentrations of [^{3}H]AdoMet were incubated for 10 min at 55 °C.

Gel Mobility Shift Assay—A gel mobility shift assay was performed according to our previous reports (30, 31).

Crystallization and X-ray Crystal Structure Study—Purified protein (10 mg/ml) in buffer B (20 mM Tris-HCl, pH 8.0, 150 mM NaCl, 2 mM dithiothreitol) was mixed with an equal volume of buffer C (100 mM sodium citrate, pH 5.5, 2 M ammonium sulfate) in the presence of 1 mM AdoMet or sinefungin (AdoMet analog) and then crystallized at 4 °C by the sitting drop method. The Trm1 crystals grew within 14 days. The crystals were flash-cooled to 100 K using liquid paraffin oil as the cryoprotectant. X-ray diffraction data were collected at the Photon Factory NW12A and BL5A beamlines for the AdoMet- and sinefungin-bound crystals, respectively, and processed with the HKL2000 program suite (32). The structures were solved with the program MOLREP (33) by molecular replacement using the *P. horikoshii* Trm1 structure (PDB code 2EJT) as a search model. The models were built with the program Coot (34) and refined with the programs CNS (35) and Phenix (36). The information of crystal data collection is given in supplemental Table 1. The R_{work}/R_{free} factors of refined coordinates of Trm1-sinefungin complex crystal structure were 0.186/0.219.

Computer Programs for Figures—The structural figures were generated by using PyMOL (DeLano Scientific, Palo Alto, CA), and the electrostatic potential surface models were calculated by using APBS (37). The schematic diagram of interaction of sinefungin with the amino acid residues in Trm1 was generated by using LIGPLOT (38). The amino acid sequence alignment was generated by using ClustalW 1.83 (39) and ESPript (40) programs.

Inductivity Coupled Plasma Emission Spectrometry—The inductivity coupled plasma emission analysis was performed by the Chemical Analysis Laboratory, University of Georgia.

RESULTS

A. aeolicus Trm1 Recognizes the T-arm Structure in tRNA—The tRNA recognition mechanisms of eukaryotic and archaeal Trm1 proteins have been well studied (9–12, 16–18). Although there are several differences in the tRNA recognition mechanisms of eukaryotic and archaeal Trm1, both enzymes recognize the D-arm structure and variable region in tRNA (Fig. 1*C*). In our previous study (21), we reported that *A. aeolicus* Trm1, a eubacterial enzyme, has a completely different tRNA recognition mechanism from those of eukaryotic and archaeal Trm1. First, *A. aeolicus* Trm1 catalyzes methyl transfers not only to G26 but also to G27 in tRNA, whereas all eukaryotic and archaeal enzymes reported thus far catalyze methyl transfer to only G26. Second, *A. aeolicus* Trm1 catalyzes methyl transfers to class II tRNAs as well as all class I tRNAs tested, showing that the size and sequence of the variable region are not recognized by *A. aeolicus* Trm1. Third, tRNA transcripts containing G26 and/or G27, which were tested in our previous study, have different D-arm structures; however, all tRNA transcripts are methylated by *A. aeolicus* Trm1. Thus, the D-arm structure is not a positive determinant for *A. aeolicus* Trm1. Fourth, truncated tRNA experiments in our previous

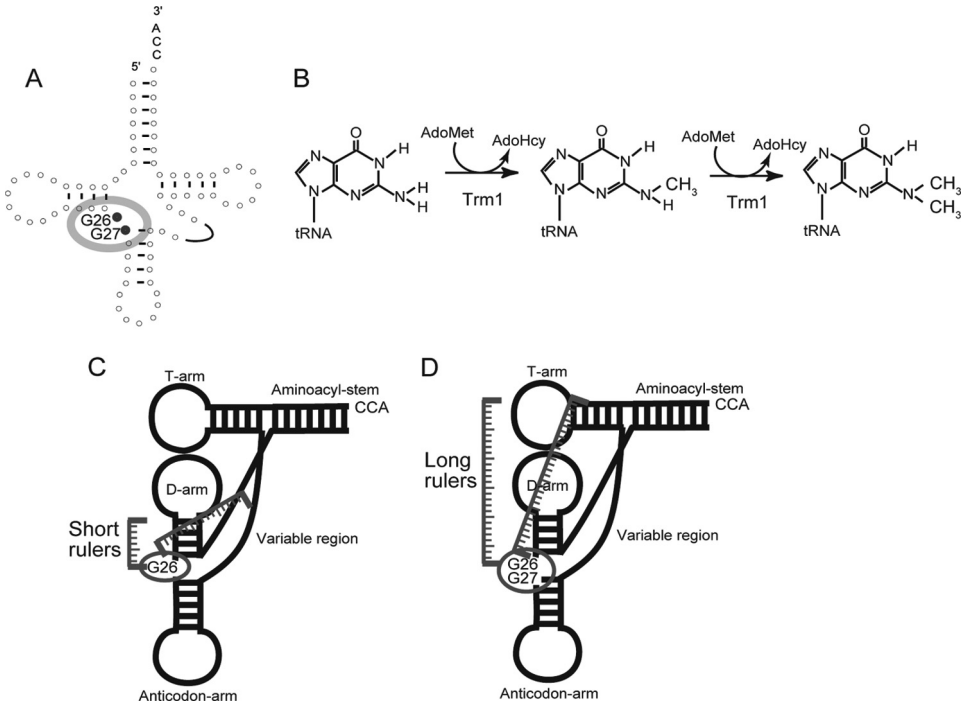

FIGURE 1. **Methylation by Trm1 enzymes.** *A,* methylation sites, G26 and G27, are highlighted in the *cloverleaf* structure of tRNA. Eukaryotic and archaeal Trm1 are single site-specific enzymes that modify only G26. In contrast, *A. aeolicus* Trm1 is a multisite-specific enzyme, which modifies both G26 and G27. *B,* Trm1 catalyzes methyl transfer to the target guanine from AdoMet, and m^2G is produced as an intermediate. AdoMet is converted to AdoHcy by the reaction. *C* and *D* are slight modifications of Fig. 9 in our previous report (21). *C,* eukaryotic and archaeal Trm1 reported thus far recognize the D-arm and variable region in tRNA. *D,* in contrast, *A. aeolicus* Trm1 is expected to recognize the T-arm structure. Thus, the distance(s) from the recognition site(s) in tRNA to the modification site(s) may affect both single and multisite specificities.

study showed that the T-arm structure is required for methylation by *A. aeolicus* Trm1. Taking these experimental results together, we proposed a long distance recognition mechanism of *A. aeolicus* Trm1 in our previous study (Fig. 1*D*).

In our hypothetical mechanism, the T-arm structure is a key region in the substrate recognition mechanism of *A. aeolicus* Trm1. To confirm this idea, here we initially performed a gel mobility shift assay with *A. aeolicus* Trm1 (Fig. 2). This gel mobility assay system was originally devised for detection of tRNA elongation factor Tu-GTP ternary complex (41, 42). Because this system was used for measurement of affinity of nematoda mitochondrial elongation factor Tu for T-armless tRNAs (41), we selected this system. One of the virtues of this system is the usage of buffer containing 5 mM $MgCl_2$ to maintain the L-shaped tRNA structure. Therefore, this gel shift system is applicable for various tRNA-related proteins. In the case of *A. aeolicus* Trm1, the enzyme does not migrate into the gel in the absence of RNA because the isoelectric point (pI) of *A. aeolicus* Trm1 is 9.06. When a full-length $tRNA^{Phe}$ transcript was used in the assay, *A. aeolicus* Trm1 clearly formed a tRNA-protein complex (Fig. 2, *A* and *B*), as visualized by double staining with methylene blue and Coomassie Brilliant Blue (Fig. 2*B*). When the D-arm structure was deleted, a similar band corresponding to the tRNA-Trm1 complex was observed (Fig. 2, *C* and *D*). In contrast, when the T-arm structure was deleted, the band corresponding to the tRNA-Trm1 complex disappeared (Fig. 2, *E* and *F*), demonstrating that the T-arm structure is indeed essential for substrate RNA binding by *A. aeolicus* Trm1. In these experiments, because the band corresponding to free tRNA was broadened in the presence of *A. aeolicus* Trm1, we avoided the calculation of K_d values.

Overall Structure of A. aeolicus Trm1—A. aeolicus Trm1 recognizes the T-arm structure in tRNA. This feature is considerably different from the mechanisms of archaeal and eukaryotic Trm1. To obtain structural information on *A. aeolicus* Trm1, we performed an x-ray crystal structure study. We have solved the structures of AdoMet-Trm1 (PDB code 3AXT) and sinefungin-Trm1 (PDB code 3AXS) complexes (supplemental Table 1). Sinefungin is an analog inhibitor, in which the activated methyl group of AdoMet is replaced by an amino group (see Fig. 5*B*) (43, 44). Because the structures of AdoMet-Trm1 and sinefungin-Trm1 complexes are almost identical and the resolution of sinefungin-Trm1 complex (2.15 Å) is better than that of the AdoMet-Trm1 complex, we performed this study based on the structure of sinefungin-Trm1 complex (Fig. 3). *A. aeolicus* Trm1 includes two domains as follows: an N-terminal Rossmann fold domain (Fig. 3, *cyan*), and a C-terminal novel structure domain (*magenta*). Although the C-terminal domain structure of *A. aeolicus* Trm1 is clearly different from that of *P. horikoshii* Trm1 (archaeal enzyme; PDB codes 2EJT and 2DUL) (19), the overall structure and topology of *A. aeolicus* Trm1 is similar to that of *P. horikoshii* Trm1 (Fig. 4). The N-terminal Rossmann fold domain is a typical catalytic domain of class I AdoMet-dependent methyltransferases. AdoMet-dependent methyltransferases are categorized into five classes based on the type of fold present in the catalytic domain (45). Here, a bound sinefungin (*yellow*) was found in the Rossmann fold domain (Figs. 3 and 4). The C-terminal domain was found to

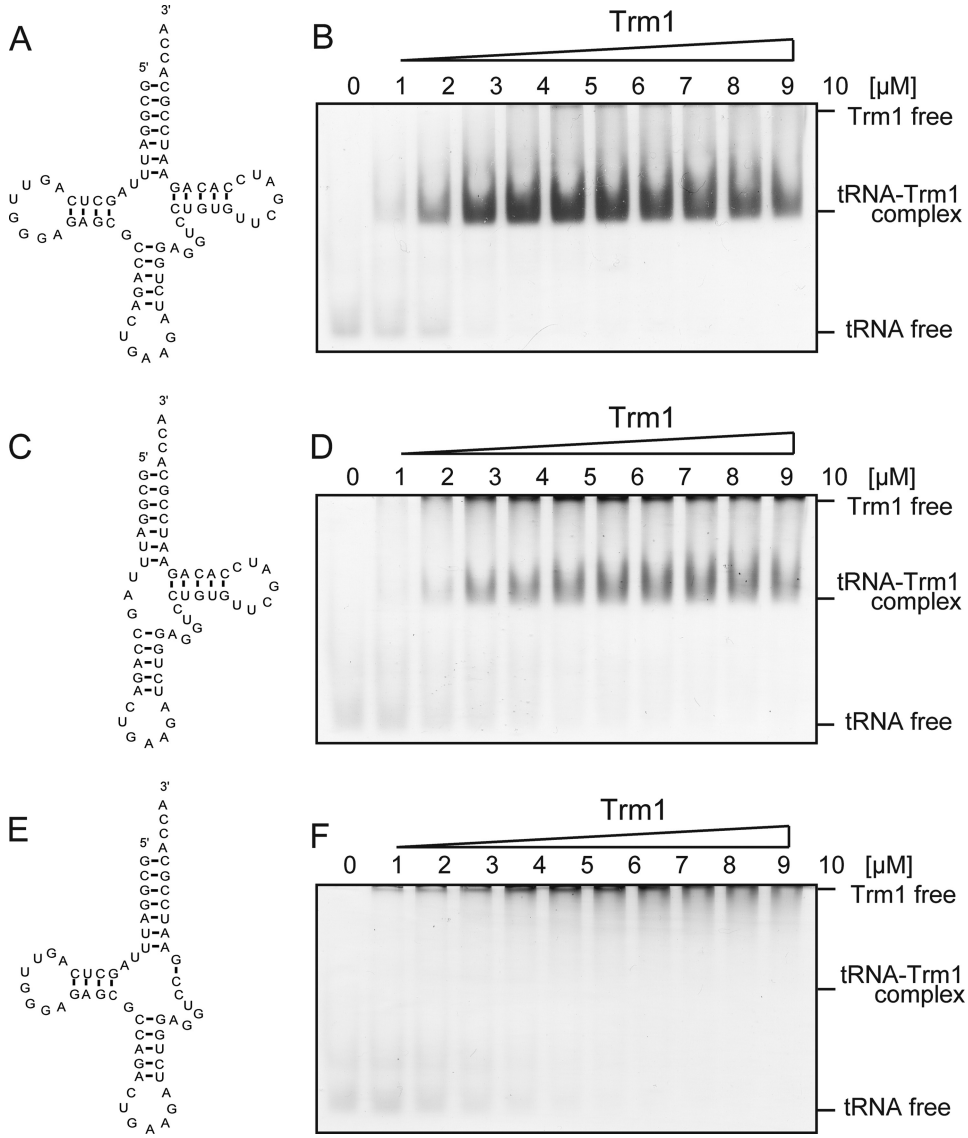

FIGURE 2. **Gel mobility shift assay with *A. aeolicus* Trm1.** *A, cloverleaf* structure of the full-length yeast $tRNA^{Phe}$ transcript. *B,* as the Trm1 concentration increased, full-length $tRNA^{Phe}$ and *A. aeolicus* Trm1 formed an RNA-protein complex. The gel was double-stained with Coomassie Brilliant Blue for the detection of protein and methylene blue for the detection of RNA. *C,* mutant $tRNA^{Phe}$ transcript, in which the D-arm was deleted. *D,* as the Trm1 concentration increased, the mutant tRNA transcript lacking the D-arm formed an RNA-protein complex although with decreased affinity. *E,* mutant $tRNA^{Phe}$ transcript, in which the T-arm was deleted. *F,* in contrast to *B* and *D*, bands corresponding to the RNA-protein complex were not observed with the mutant tRNA transcript lacking the D-arm, although bands corresponding to tRNA free were broadened with the increase in Trm1 concentration.

have a novel structure, in which one zinc atom (Fig. 4, *orange*) was bound to four cysteine residues (Cys-247, Cys-250, Cys-266, and Cys-269) (Figs. 3 and 4). Furthermore, four sulfate ions were bound to *A. aeolicus* Trm1; one sulfate ion was bound to the His-110 residue in the N-terminal domain, and three sulfate ions were bound to the border area between the N- and C-terminal domains (Fig. 3). These sulfate ions seemed to bind Trm1 instead of the phosphate groups in tRNA.

Structure-based Amino Acid Sequence Alignment and Target Residues of Site-directed Mutagenesis—On the basis of the structural information, we aligned the amino acid sequences of the Trm1 proteins reported thus far (supplemental Fig. 1). Although the tRNA recognition mechanism of *A. aeolicus* Trm1 differs from those of eukaryotic and archaeal Trm1, the amino acid sequence of *A. aeolicus* Trm1 seems to be an intermediate of those of eukaryotic and archaeal Trm1. For example, *A. aeolicus* Trm1 lacks a long stretch between the α1 helix and β3 strand in the N-terminal region of eukaryotic enzymes; this is a feature of archaeal enzymes. However, *A. aeolicus* Trm1 has a cysteine cluster (*green* in Fig. 4 and supplemental Fig. 1), which is observed only in eukaryotic enzymes. Furthermore, the intervening sequence between β11 and β12 of *A. aeolicus* Trm1 is shorter than that of eukaryotic enzymes.

To predict the reaction mechanism and substrate-binding sites, we introduced single alanine and serine substitutions into *A. aeolicus* Trm1. The target sites (Fig. 4 and *triangles* and *stars* in supplemental Fig. 1) were selected on the basis of the crystal structure and amino acid sequence alignment. We performed site-directed mutagenesis and prepared 30 mutant Trm1 proteins. All mutant Trm1 proteins were purified to near-homogeneity, as judged by 15% SDS-PAGE (supplemental Fig. 2).

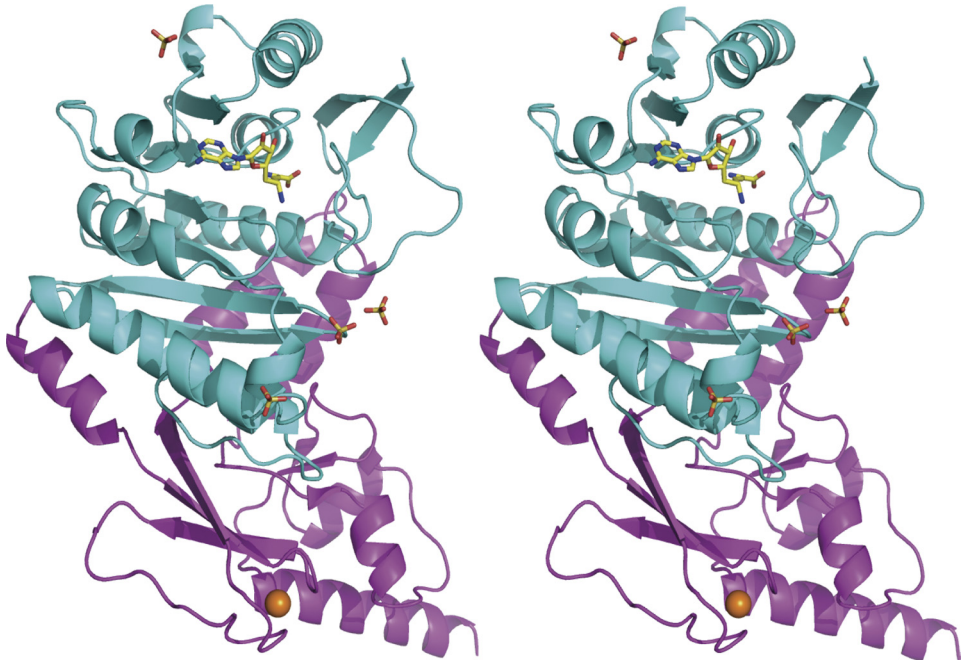

FIGURE 3. **Stereo view of the overall structure of *A. aeolicus* Trm1.** *A. aeolicus* Trm1 includes an N-terminal catalytic domain (*cyan*) and a C-terminal domain (*magenta*). Bound sinefungin (*yellow*) is highlighted by a *stick* model. Four sulfate ions are also shown by a *stick* model. An *orange ball* represents a zinc atom.

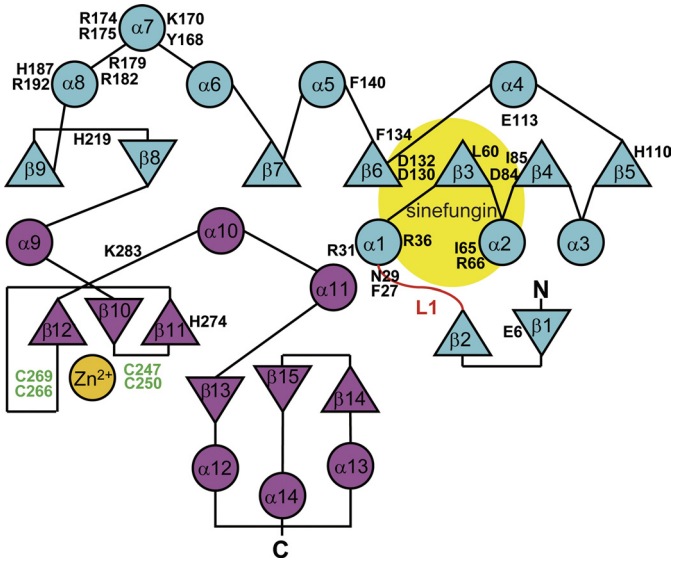

FIGURE 4. **Topology of *A. aeolicus* Trm1 and mutation sites.** Topology of *A. aeolicus* Trm1 is schematically drawn. The α-helices and β-strands are shown by *circles* and *triangles*, respectively. The L1-loop is highlighted in *red*. An *orange circle* shows the bound zinc atom. The N- and C-terminal domains are indicated in *cyan* and *magenta*, respectively. Amino acid residues are the mutation sites.

AdoMet-binding Site and Hypothetical Reaction Mechanism—Fig. 5*A* shows the AdoMet-binding site in the N-terminal catalytic domain. A conserved aspartic acid (Asp-132) residue is located near the amino group of sinefungin, which corresponds to the methyl group of AdoMet. This residue was expected to be the catalytic center of *A. aeolicus* Trm1 on the basis of the amino acid sequence alignment and crystal structure (Fig. 4) (19, 21). Indeed, alanine substitution of Asp-132 caused a complete loss of methyl transfer activity (Table 1), consistent with the idea that Asp-132 is the catalytic center. In the crystal structure, the carboxyl group of Asp-132 forms a hydrogen bond with the Arg-66 residue (Fig. 5*B*). The alanine substitution mutant of Arg-66 showed a severe loss of methyl transfer activity (1:1000 of the wild-type enzyme) (Table 1). This loss was probably due to two reasons. One is that the guanidino group of Arg-66 functions as a part of the electron relay system. The other is that the hydrogen bond between Arg-66 and Asp-132 determines the direction of the carboxyl group of Asp-132 (predicted catalytic center). Arg-66 forms a hydrogen bond with another aspartic acid (Asp-130) (Fig. 5*A*). Asp-130 is highly conserved (Fig. 4) and does not contact AdoMet directly. The alanine substitution of this residue caused an increase in K_m values for AdoMet. Therefore, Asp-130 seems to contribute to the formation of AdoMet binding pocket to contact Arg-66. There are two conserved phenylalanine residues (Phe-27 and Phe-134) located near the amino group of sinefungin (Fig. 5, *A* and *B*). The alanine substitution mutant of Phe-27 showed a severe loss of methyl transfer activity (1:400 of the wild-type enzyme) through an increase in the K_m value and a decrease in the V_{max} value for AdoMet (Table 1). Phe-27 may have two functions because it is located in the flexible loop region (L1-loop). First, the Phe-27 is a part of the AdoMet-binding site through a hydrophobic interaction between Phe-27 and the methionine of AdoMet because the K_m value for AdoMet was increased more than 100-fold as compared with the wild-type enzyme. Second, Phe-27 may fix the target guanine (G26 or G27) by a hydrophobic interaction in the presence of tRNA. However, we could not measure the kinetic parameters of the F27A mutant for tRNA (data not shown); the methyl transfer activity was too low to calculate the values, and two-dimensional TLC analysis showed that second methylation ($m^2{}_2$G26 formation) occurred in the low concentration samples (data not shown). Therefore, we could not conclude whether Phe-27 is responsible for tRNA (guanine) binding, although it is the most likely candidate for guanine binding. The importance of Phe-27

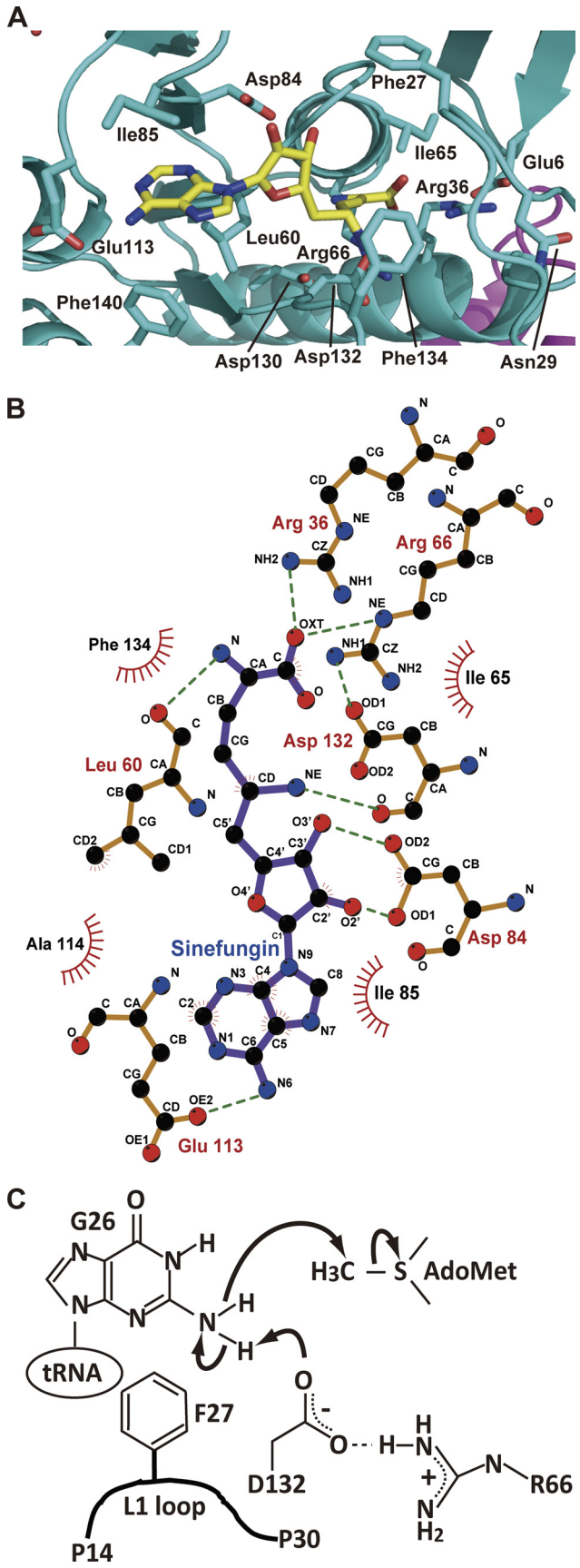

FIGURE 5. **AdoMet-binding site and hypothetical reaction mechanism.** *A,* structure of AdoMet-binding site and bound sinefungin. Amino acid residues around the AdoMet-binding site and sinefungin are highlighted by *stick* models. *B,* interactions between amino acid residues and sinefungin. *C,* hypothetical catalytic mechanism. The catalytic center is the Asp-132 residue. As described in the text, the Arg-66 residue contributes to the electron relay pathway. The activated amino group of G26 in tRNA attacks the methyl group of AdoMet. Phe-27 in the L1-loop probably contributes to fixation of the target guanine base by a hydrophobic interaction.

TABLE 1
Kinetic parameters for AdoMet

ND means that methyl transfer activity is not detectable. The relative K_m/V_{max} value is expressed that of the wild type enzyme as 1.00.

Alanine substitution, mutant name	K_m	V_{max}	Relative V_{max}/K_m
	nM	*nmol mg*$^{-1}$ *h*$^{-1}$	
Wild type	170	90	1.00
Glu-6	300	130	0.84
Phe-27[a]	>23,000	30–100	<0.0025
Asn-29	300	90	0.57
Arg-36	ND	ND	ND
Leu-60	670	170	0.49
Ile-65	200	170	1.70
Arg-66[a]	>45,000	30–100	<0.0011
Asp-84[a]	>330,000	100–200	<0.0012
Ile-85	170	50	0.51
Glu-113	670	170	0.49
Asp-130	1300	170	0.25
Asp-132	ND	ND	ND
Phe-134	800	260	0.65
Phe-140	670	430	1.30

[a] Kinetic parameters for these mutants could not be measured correctly because of low methyl transfer activities.

residue in the L1-loop was also previously reported for *P. horikoshii* Trm1 (19). In contrast, alanine substitution of Phe-134 did not cause a significant effect; the methyl transfer activity was decreased to a third of the level of the wild-type enzyme through an increase in K_m and a decrease in V_{max} values (Table 1), suggesting that Phe-134 is a structural element of the AdoMet-binding site. This result is different from previous results with the *P. horikoshii* Trm1 mutant protein (19). In the case of *P. horikoshii* Trm1, the substitution of Phe-140, which corresponds to Phe-134 in *A. aeolicus* Trm1, by alanine caused a severe loss of methyl transfer activity (19). Thus, structural contribution of this phenylalanine (Phe-134 in *A. aeolicus* Trm1) residue to the architecture of catalytic pocket seems to differ in Trm1 proteins. Taken together, these results enable us to predict a hypothetical reaction mechanism of *A. aeolicus* Trm1 (Fig. 5*C*). In this mechanism, the role of Phe-27 is not clear, although its location suggests that this residue fixes the guanine base in tRNA by a hydrophobic interaction. Furthermore, the result of alanine substitution did not contradict the idea that the Asp-132 is a catalytic center.

As shown in Fig. 5, *A* and *B*, sinefungin forms hydrogen bonds with many amino acid residues in the catalytic domain. These interactions were also observed in the AdoMet-*P. horikoshii* Trm1 complex (19). The amino group of adenine of sinefungin forms a hydrogen bond with one glutamic acid (Glu-113). In the case of *P. horikoshii* Trm1, this glutamic acid is replaced by an aspartic acid (Asp-120). Thus, this interaction between an acidic amino acid and amino group of adenine is conserved. However, substitution of Glu-113 by alanine did not have a significant effect, showing that the Glu-113 is a weak AdoMet-binding site. One isoleucine residue (Ile-85) hydrophobically interacts with the adenine of sinefungin; however, alanine substitution of Ile-85 did not cause a severe effect,

showing that Ile-85 is also a weak AdoMet-binding site. The ribose of sinefungin contacts one conserved aspartic acid residue (Asp-84), and alanine substitution of Asp-84 caused a severe decrease of methyl transfer activity (1:1000 of the wild-type enzyme) through an increase in the K_m value for AdoMet. Thus, Asp-84 is very important for AdoMet binding and, in fact, is highly conserved in Trm1 proteins (supplemental Fig. 1). The carboxyl group of methionine of sinefungin formed a hydrogen bond with the Arg-36 residue. Disruption of this interaction by alanine substitution brought a severe loss of methyl transfer activity (1:1000) through an increase in K_m values for AdoMet, demonstrating that Arg-36 is also very important for AdoMet binding. Arg-36 residue forms a hydrogen bond with a semi-conserved glutamic acid (Glu-6), which constitutes half of a distinctive amino acid sequence motif, the so-called "EG motif" (19, 46). Because the EG motif forms a sharp β-turn and is located near the AdoMet-binding site, it has been predicted to be involved in the catalytic mechanism (19, 46). Furthermore, it has been reported that the deletion of the EG motif in *S. cerevisiae* Trm1 causes complete loss of the enzymatic activity (47). However, alanine substitution of Glu-6 did not have an effect on methyl transfer activity. Thus, this result revealed that the Glu-6 residue itself is not involved in the catalytic mechanism. Taking these results together, we conclude that AdoMet mainly binds to Trm1 by hydrogen bonds. In general, a hydrogen bond is weakened at high temperatures. Even though *A. aeolicus* is a hyper-thermophile, this AdoMet-binding mode, which is a typical feature of class I AdoMet-dependent methyltransferases (43), is conserved. This AdoMet-binding mode is completely different from that of class IV enzymes such as TrmH; in the case of TrmH, for example, AdoMet binds to the enzyme hydrophobically (30, 48).

Use of Alanine Substitution Mutants to Search for the tRNA-binding Site—As described above, four sulfate ions were found on the surface of *A. aeolicus* Trm1 because we used ammonium sulfate for crystallization. We assumed that some of these sulfate ions occupied the phosphate (tRNA)-binding sites. We therefore selected 13 amino acid residues (Arg-31, His-110, Tyr-168, Lys-170, Arg-174, Arg-175, Arg-179, Arg-182, His-187, Arg-192, His-219, His-274, and Lys-283; marked by *stars* in supplemental Fig. 1) to test tRNA binding on the basis of the sulfate ion positions and amino acid sequence alignment. In general, searching for a tRNA-binding site by alanine substitution is not so easy because a single mutation does not bring the severe loss of methyl transfer activity observed in the search for the catalytic center and AdoMet-binding site (49). Nevertheless, our alanine substitution experiments identified residues important for tRNA binding as follows: alanine substitutions of eight residues (Arg-31, His-110, Lys-170, Arg-179, Arg-192, His-219, His-274, and Lys-283) led to a clear decrease in methyl transfer activity and, in particular, the alanine substitution mutants of Arg-179 and His-219 showed a significant decrease in the methyl transfer activity (Fig. 6*A*). To confirm whether Arg-179 and His-219 residues are part of the tRNA-binding site or not, we performed a gel mobility shift assay (Fig. 6*B*). Both alanine substitution mutants (R179A and H219A) showed a decrease in affinity for the tRNA transcript. Thus, we confirmed that Arg-179 and His-219 are important for tRNA binding and that Arg-31, His-110, Lys-170, Arg-192, His-274, and Lys-283 probably form part of the tRNA-binding site.

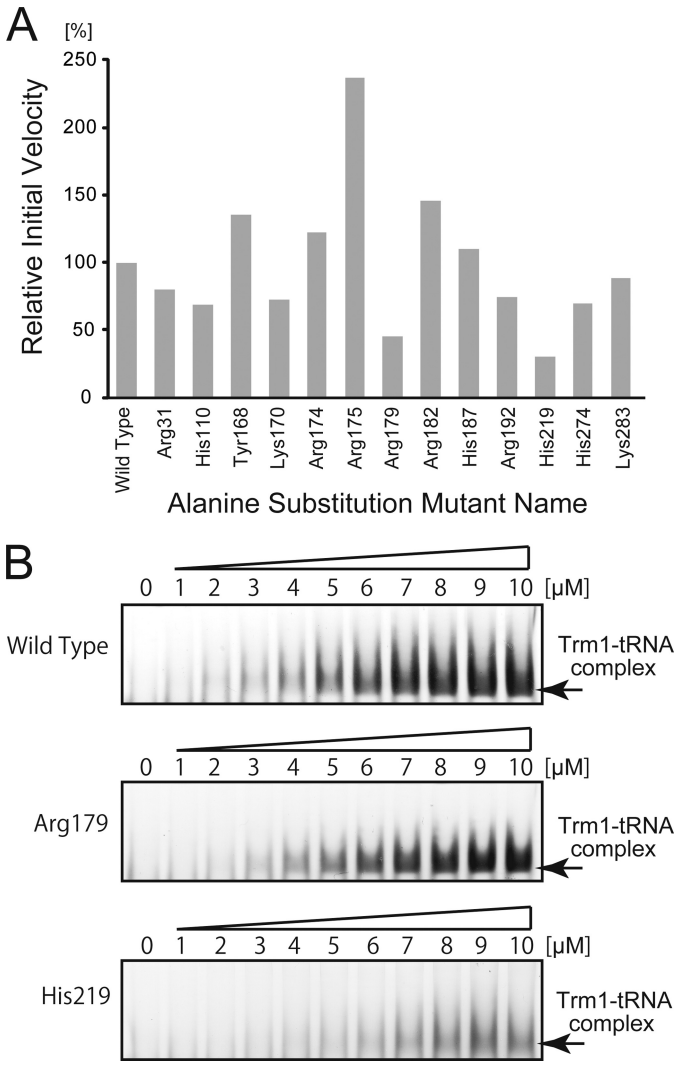

FIGURE 6. **Determination of tRNA-binding site by site-directed mutagenesis.** *A,* methyl transfer activity of the alanine-substituted mutant proteins. The mutant name indicates the site of alanine substitution. The initial velocity of wild-type Trm1 is expressed as 100%. Data are the average of four independent experiments. *B,* gel mobility shift assay of wild-type Trm1 (*upper panel*), the alanine substitution mutant of Arg-179 (*middle panel*), and the alanine substitution mutant of His-219 (*lower panel*). As the protein concentration increased, the protein-tRNA complex was formed. However, the Arg-179 and His-219 mutants have weaker affinity for the yeast $tRNA^{Phe}$ transcript as compared with the wild-type enzyme.

Zinc Atom and Cysteine Cluster—As described above, one zinc atom was bound to four cysteine residues (Cys-247, Cys-250, Cys-266, and Cys-269). The bound metal was identified as zinc by x-ray absorption fluorescence spectroscopic analysis and inductivity coupled plasma emission analysis (data not shown), and its position was consistent with the cysteine cluster motif (50, 51). It should be mentioned that zinc binding by this cysteine cluster was previously predicted by a bioinformatics study by Bujnicki *et al.* (46). Thus, this study is in good agreement with their bioinformatics study (46). Because this zinc atom is located in the C-terminal domain far from the catalytic center, we considered that the zinc atom and cysteine cluster comprise a structural element of the C-terminal domain. To

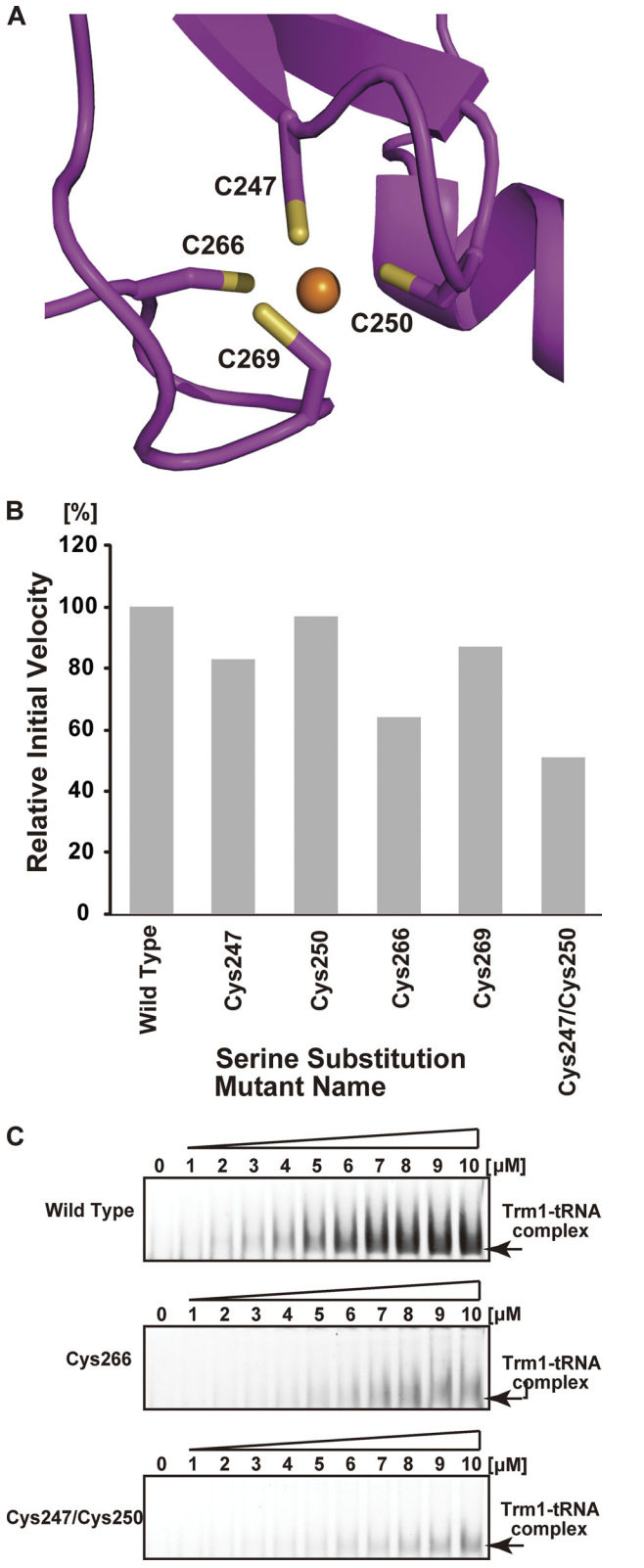

FIGURE 7. **Cysteine cluster mutants.** *A,* structure of the cysteine cluster chelating a zinc atom. Sulfur atoms and the zinc atom are indicated in *yellow* and *orange*, respectively. *B,* comparison of methyl transfer activities of the serine substitution mutants with that of the wild-type Trm1. The initial velocity of wild-type Trm1 is expressed as 100%. Data are the average of four independent experiments. *C,* gel mobility shift assay of the wild-type Trm1 (*upper panel*), the serine substitution mutant of Cys-266 (*middle panel*), and the double serine substitution mutant of Cys-247 and Cys-250 (*lower panel*). Disruption of the zinc-cysteine cluster causes a severe decrease in affinity for tRNA.

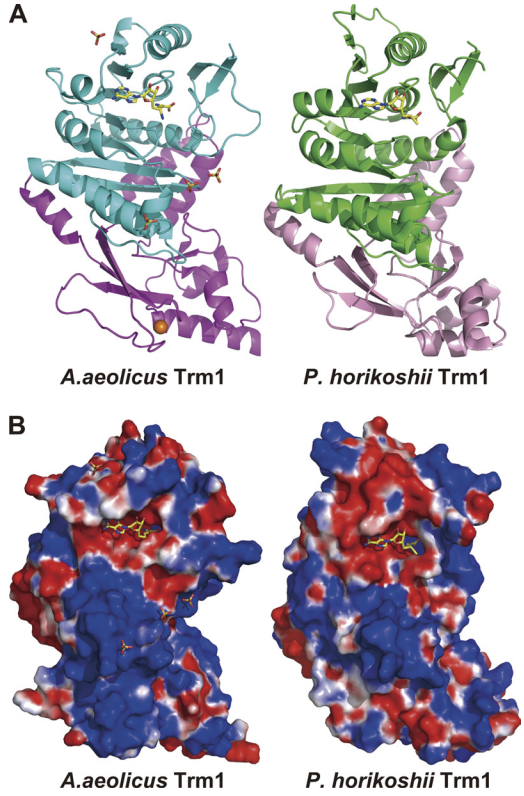

FIGURE 8. **Comparison of *A. aeolicus* Trm1 with archaeal Trm1 (*P. horikoshii* Trm1).** *A,* comparison of the structures of the two proteins. As described in the text, *A. aeolicus* Trm1 (*left panel*) has a multisite specificity and modifies both G26 and G27 in tRNA. In contrast, *P. horikoshii* Trm1 (*right panel*) has single site specificity and modifies only G26 in tRNA. Although *A. aeolicus* Trm1 has a zinc-cysteine cluster in the C-terminal domain, the overall structures of both proteins are similar. The catalytic domains (*cyan* in *A. aeolicus* Trm1 and *green* in *P. horikoshii* Trm1) are almost identical. *B,* in contrast, comparison of the electrostatic potential surface models of both proteins shows that the electric charges of the protein surfaces are considerably different. *A. aeolicus* Trm1 has a large area of positive charge at the border between the N- and C-terminal domains (*left panel*). In contrast, the area of positive charge in *P. horikoshii* Trm1 is relatively small (*right panel*).

confirm this idea, we performed serine substitution of four cysteine residues individually (*green* in Figs. 4 and 7*A*). As shown in Fig. 7*B*, serine substitution of each cysteine residue caused a decrease in methyl transfer activity. However, considerable activity remained; for example, the C250S mutant had more than 90% of the activity of the wild-type enzyme. Therefore, we considered that single mutations might not disrupt the zinc-bound cysteine cluster completely. To test the stability of the cluster, we dialyzed the wild-type enzyme against buffer A containing 10 mM EDTA at 4 °C overnight; however, no loss of activity was observed (data not shown). Furthermore, after incubation of the wild-type enzyme with 50 mM EDTA at 90 °C for 30 min, more than 90% of the methyl transfer activity remained (data not shown). Thus, the zinc-cysteine cluster is considerably stable. We therefore prepared a double-mutated Trm1 (C247S and C250S) protein to disrupt the cluster. As expected, this mutant protein showed a significant decrease in activity (Fig. 7*A*). Furthermore, the gel mobility shift assay showed a decrease in affinity of the double-mutated protein for tRNA (Fig. 7*B*). On the basis of these results, we concluded that the cysteine cluster is a structural element that maintains the tRNA-binding site between the N- and C-terminal domains.

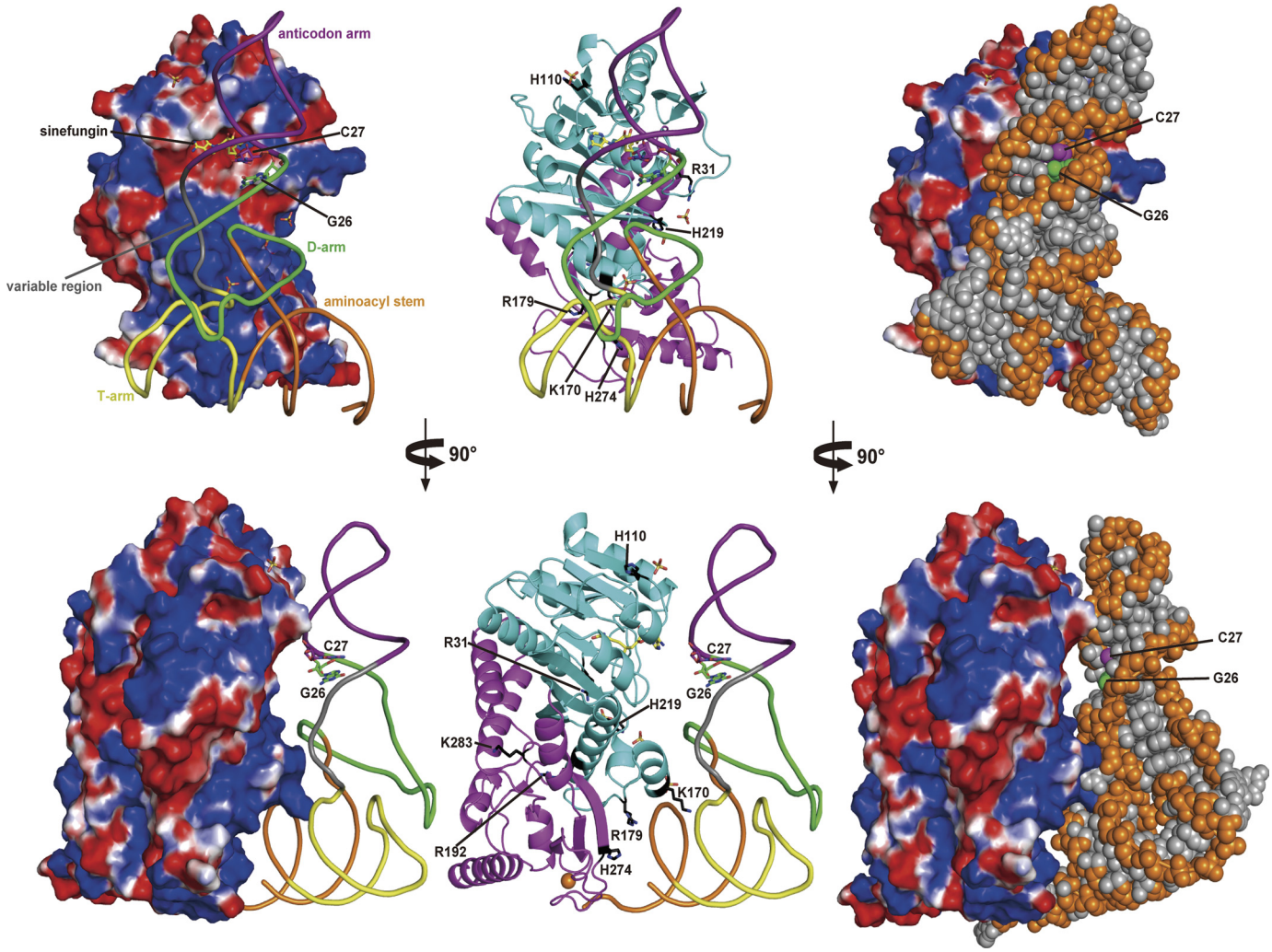

FIGURE 9. **Model of tRNA docking on *A. aeolicus* Trm1.** Yeast $tRNA^{Phe}$ (phosphate-ribose backbone) was docked onto the expected tRNA-binding site in the *A. aeolicus* Trm1. The G26 and C27 bases are highlighted by *stick models*. In the docking model, we placed the T-arm at the border region between the N- and C-terminal domains. The *right panel* shows the space-filling model of tRNA. The target G26 base can be placed near the catalytic pocket; however, the C27 base gains closer access to the pocket in the model. If the anticodon stem structure (*i.e.* the base pair between nucleotides at positions 27 and 43) is disrupted in the Trm1-tRNA complex, the docking model suggests that tRNA species with G27 could be modified by *A. aeolicus* Trm1. *Lower panels* show a side view of the model after a 90° anticlockwise rotation.

Comparison of A. aeolicus Trm1 with Archaeal Trm1 and tRNA Docking Model—Finally, we compared *A. aeolicus* Trm1 with *P. horikoshii* Trm1 (archaeal enzyme). As shown in Fig. 8*A*, the apparent overall structures of both Trm1 proteins resemble each other. However, the electrostatic potential surface models of the two proteins show that the electric charges on the protein surfaces are considerably different (Fig. 8*B*). In the case of *A. aeolicus* Trm1 (Fig. 8*B, left*), there is a broad positive charge area at the border between the N- and C-terminal domains. The amino acid residues (Lys-170, Arg-179, Arg-182, His-187, and His-219) involved in tRNA binding are present in this area. In fact, three sulfate ions were found in this region. In the case of *P. horikoshii* Trm1 (Fig. 8*B, right*), by contrast, the area of positive charge is observed only around the catalytic pocket; instead, a lot of negative charge exists around the border area between the N- and C-terminal domains. These differences in the distribution of positive charge suggest that the tRNA-binding mode differs between the *A. aeolicus* and *P. horikoshii* Trm1 proteins.

To address the tRNA-binding mode of *A. aeolicus* Trm1, we constructed a tRNA-docking model, in which the T-arm region of yeast $tRNA^{Phe}$ was manually placed at the border between the N- and C-terminal domains, *i.e.* at the expected tRNA-binding site (Fig. 9). This model explains why *A. aeolicus* Trm1 catalyzes methyl transfers to G27, as well as G26. In the model, the catalytic pocket of *A. aeolicus* Trm1 can be placed near G26 in tRNA. However, another target guanine, G27 (C27 in the model), is positioned closer to the catalytic pocket than G26. If the anticodon stem structure is disrupted according to the formation of a tRNA-Trm1 complex, then G27 will be more accessible to the catalytic center than G26. Thus, the T-arm recognition and G27 methylation of *A. aeolicus* Trm1 are explainable by the distributions of positive charge determined from our structural study.

DISCUSSION

In this study, we have focused on the multisite specificity of *A. aeolicus* Trm1, a eubacterial enzyme, which recognizes the T-arm structure of tRNA. Our x-ray crystal structural study has revealed that the apparent overall structure of *A. aeolicus* Trm1 is similar to that of *P. horikoshii* Trm1 (archaeal enzyme),

although the *A. aeolicus* Trm1 has a novel C-terminal domain with a zinc atom. On the basis of the crystal structure and amino acid sequence alignment, we have performed a site-directed mutagenesis study, enabling us to propose a hypothetical reaction mechanism of *A. aeolicus* Trm1 and to determine the amino acid residues responsible for AdoMet binding. Our hypothetical reaction mechanism seems to be reasonable for an amino group methyltransferase (19, 52). The AdoMet-binding site is typical of class I AdoMet-dependent methyltransferases (45).

We have also predicted the tRNA-binding site by the site-directed mutagenesis study based on the sulfate ion binding in the crystal structure and amino acid sequence alignment. The amino acid residues involved in tRNA binding mainly map to the border area between the N- and C-terminal domains. The electrostatic potential surface model of *A. aeolicus* Trm1 has demonstrated that the border area between the N- and C-terminal domains forms a large area of positive charge, which is not observed in the model of *P. horikoshii* Trm1. The tRNA docking model of *A. aeolicus* Trm1, in which the T-arm was placed at the border area between the N- and C-terminal domains, has elucidated the multisite recognition mechanism of *A. aeolicus* Trm1 by showing that G27 can be placed closer to the catalytic pocket than G26. Among multisite-specific tRNA modification enzymes, *Escherichia coli* TruA modifies U38, U39, and U40 to Ψ38, Ψ39, and Ψ40, respectively (53, 54), and is the only enzyme whose multisite recognition mechanism has been studied by the tRNA-enzyme complex (55). In this study, we have been able to propose a hypothetical mechanism for the multisite specificity of *A. aeolicus* Trm1; however, a structural study of tRNA-Trm1 complex will be necessary, like that of TruA, for a discussion of the detailed mechanism.

The multisite specificity and tRNA recognition mode of *A. aeolicus* Trm1 is completely different from those of eukaryotic and archaeal Trm1, although *A. aeolicus* Trm1 seems to be an intermediate of eukaryotic and archaeal Trm1 proteins from the amino acid sequence alignment. These facts suggest that the RNA recognition mechanism of RNA modification enzymes may have changed during molecular evolution process, even though the enzymes bring about the same modification(s) at the same position(s) in RNA. In another case of single- and multisite specific enzymes, eubacterial TrmI modifies only A58 in the T-loop of tRNA (56, 57), whereas archaeal TrmI modifies both A57 and A58 (22). The RNA recognition mechanisms of eubacterial and archaeal TrmI may differ from each other, although both enzymes share structural relationships (57, 58). In fact, it has been recently reported that the *P. abyssi* (archaeal) TrmI requires the A59 sequence for A58 methylation in tRNA, whereas *Thermus thermophilus* (eubacterial) TrmI does not require the A59 (58). Furthermore, in their report, the A59 requirement of archaeal TrmI is structurally revealed; the His-78 residue is involved in the A59 recognition (58). It should be mentioned that the eukaryotic counterpart of m^1A58 methylation in tRNA is a hetero-subunit enzyme, Trm6 (gcd10-gcd14 complex in yeast) (59, 60). In the case of m^1A58 modification, the eukaryotic enzyme probably has a different RNA recognition mechanism from those of the eubacterial and archaeal TrmI enzymes. To verify this idea, further studies will be necessary. In addition, this study has revealed that the RNA recognition mechanism cannot be simply predicted by an amino acid sequence alignment. Combined use of biochemical approaches and structural studies is required for full understanding of the RNA recognition mechanism.

Acknowledgment—We thank Madoka Nishimoto (RIKEN Yokohama, Systems and Structural Biology Center) for technical support with crystallization.

REFERENCES

1. Rozenski, J., Crain, P. F., and McCloskey, J. A. (1999) *Nucleic Acids Res.* **27,** 196–197
2. Dunin-Horkawicz, S., Czerwoniec, A., Gajda, M. J., Feder, M., Grosjean, H., and Bujnicki, J. M. (2006) *Nucleic Acids Res.* **34,** D145–D149
3. Garcia, G. A., and Goodenough-Lashhua, D. M. (1998) in *Modification and Editing of RNA* (Grosjean, H., and Benne, R., eds) pp. 555–560, American Society for Microbiology, Washington, D. C.
4. Reinhart, M. P., Lewis, J. M., and Leboy, P. S. (1986) *Nucleic Acids Res.* **14,** 1131–1148
5. Constantinesco, F., Motorin, Y., and Grosjean, H. (1999) *J. Mol. Biol.* **291,** 375–392
6. Kuchino, Y., and Nishimura, S. (1970) *Biochem. Biophys. Res. Commun.* **40,** 306–313
7. Glick, J. M., Averyhart, V. M., and Leboy, P. S. (1978) *Biochim. Biophys. Acta* **518,** 158–171
8. Stange, N., and Beier, H. (1987) *EMBO J.* **6,** 2811–2818
9. Edqvist, J., Grosjean, H., and Stråby, K. B. (1992) *Nucleic Acids Res.* **20,** 6575–6581
10. Edqvist, J., Blomqvist, K., and Stråby, K. B. (1994) *Biochemistry* **33,** 9546–9551
11. Grosjean, H., Edqvist, J., Stråby, K. B., and Giegé, R. (1996) *J. Mol. Biol.* **255,** 67–85
12. Constantinesco, F., Motorin, Y., and Grosjean, H. (1999) *Nucleic Acids Res.* **27,** 1308–1315
13. Phillips, J. H., and Kjellin-Stråby, K. (1967) *J. Mol. Biol.* **26,** 509–518
14. Ellis, S. R., Morales, M. J., Li, J. M., Hopper, A. K., and Martin, N. C. (1986) *J. Biol. Chem.* **261,** 9703–9709
15. Niederberger, C., Gräub, R., Costa, A., Desgrès, J., and Schweingruber, M. E. (1999) *FEBS Lett.* **464,** 67–70
16. Liu, J., Zhou, G. Q., and Stråby, K. B. (1999) *Gene* **226,** 73–81
17. Liu, J., and Strâby, K. B. (2000) *Nucleic Acids Res.* **28,** 3445–3451
18. Constantinesco, F., Benachenhou, N., Motorin, Y., and Grosjean, H. (1998) *Nucleic Acids Res.* **26,** 3753–3761
19. Ihsanawati, Nishimoto, M., Higashijima, K., Shirouzu, M., Grosjean, H., Bessho, Y., and Yokoyama, S. (2008) *J. Mol. Biol.* **383,** 871–884
20. Grosjean, H., Gaspin, C., Marck, C., Decatur, W. A., and de Crécy-Lagard, V. (2008) *BMC Genomics* **9,** 470
21. Awai, T., Kimura, S., Tomikawa, C., Ochi, A., Ihsanawati, Bessho, Y., Yokoyama, S., Ohno, S., Nishikawa, K., Yokogawa, T., Suzuki, T., and Hori, H. (2009) *J. Biol. Chem.* **284,** 20467–20478
22. Roovers, M., Wouters, J., Bujnicki, J. M., Tricot, C., Stalon, V., Grosjean, H., and Droogmans, L. (2004) *Nucleic Acids Res.* **32,** 465–476
23. Motorin, Y., and Grosjean, H. (1999) *RNA* **5,** 1105–1118
24. Auxilien, S., El Khadali, F., Rasmussen, A., Douthwaite, S., and Grosjean, H. (2007) *J. Biol. Chem.* **282,** 18711–18721
25. Pintard, L., Lecointe, F., Bujnicki, J. M., Bonnerot, C., Grosjean, H., and Lapeyre, B. (2002) *EMBO J.* **21,** 1811–1820
26. Takeda, H., Toyooka, T., Ikeuchi, Y., Yokobori, S., Okadome, K., Takano, F., Oshima, T., Suzuki, T., Endo, Y., and Hori, H. (2006) *Genes Cells* **11,** 1353–1365
27. Keith, G. (1995) *Biochimie* **77,** 142–144
28. Robertus, J. D., Ladner, J. E., Finch, J. T., Rhodes, D., Brown, R. S., Clark, B. F., and Klug, A. (1974) *Nature* **250,** 546–551
29. Kim, S. H., Sussman, J. L., Suddath, F. L., Quigley, G. J., McPherson, A.,

Wang, A. H., Seeman, N. C., and Rich, A. (1974) *Proc. Natl. Acad. Sci. U.S.A.* **71,** 4970–4974
30. Watanabe, K., Nureki, O., Fukai, S., Ishii, R., Okamoto, H., Yokoyama, S., Endo, Y., and Hori, H. (2005) *J. Biol. Chem.* **280,** 10368–10377
31. Ochi, A., Makabe, K., Kuwajima, K., and Hori, H. (2010) *J. Biol. Chem.* **285,** 9018–9029
32. Otwinowski, Z., and Minor, W. (1997) *Methods Enzymol.* **276,** 307–326
33. Vagin, A., and Teplyakov, A. (2010) *Acta Crystallogr. D Biol. Crystallogr.* **66,** 22–25
34. Emsley, P., Lohkamp, B., Scott, W. G., and Cowtan, K. (2010) *Acta Crystallogr. D Biol. Crystallogr.* **66,** 486–501
35. Brünger, A. T., Adams, P. D., Clore, G. M., DeLano, W. L., Gros, P., Grosse-Kunstleve, R. W., Jiang, J. S., Kuszewski, J., Nilges, M., Pannu, N. S., Read, R. J., Rice, L. M., Simonson, T., and Warren, G. L. (1998) *Acta Crystallogr. D Biol. Crystallogr.* **54,** 905–921
36. Adams, P. D., Afonine, P. V., Bunkóczi, G., Chen, V. B., Davis, I. W., Echols, N., Headd, J. J., Hung, L. W., Kapral, G. J., Grosse-Kunstleve, R. W., McCoy, A. J., Moriarty, N. W., Oeffner, R., Read, R. J., Richardson, D. C., Richardson, J. S., Terwilliger, T. C., and Zwart, P. H. (2010) *Acta Crystallogr. D Biol. Crystallogr.* **66,** 213–221
37. Baker, N. A., Sept, D., Joseph, S., Holst, M. J., and McCammon, J. A. (2001) *Proc. Natl. Acad. Sci. U.S.A.* **98,** 10037–10041
38. Wallace, A. C., Laskowski, R. A., and Thornton, J. M. (1995) *Protein Eng.* **8,** 127–134
39. Thompson, J. D., Higgins, D. G., and Gibson, T. J. (1994) *Nucleic Acids Res.* **22,** 4673–4680
40. Gouet, P., Courcelle, E., Stuart, D. I., and Métoz, F. (1999) *Bioinformatics* **15,** 305–308
41. Ohtsuki, T., Sakurai, M., Sato, A., and Watanabe, K. (2002) *Nucleic Acids Res.* **30,** 5444–5451
42. Doi, Y., Ohtsuki, T., Shimizu, Y., Ueda, T., and Sisido, M. (2007) *J. Am. Chem. Soc.* **129,** 14458–14462
43. Pugh, C. S., Borchardt, R. T., and Stone, H. O. (1978) *J. Biol. Chem.* **253,** 4075–4077
44. Vedel, M., and Robert-Géro, M. (1981) *FEBS Lett.* **128,** 87–89
45. Schubert, H. L., Blumenthal, R. M., and Cheng, X. (2003) *Trends Biochem. Sci.* **28,** 329–335
46. Bujnicki, J. M., Leach, R. A., Debski, J., and Rychlewski, L. (2002) *J. Mol. Microbiol. Biotechnol.* **4,** 405–415
47. Liu, J., Liu, J., and Stråby, K. B. (1998) *Nucleic Acids Res.* **26,** 5102–5108
48. Nureki, O., Watanabe, K., Fukai, S., Ishii, R., Endo, Y., Hori, H., and Yokoyama, S. (2004) *Structure* **12,** 593–602
49. Watanabe, K., Nureki, O., Fukai, S., Endo, Y., and Hori, H. (2006) *J. Biol. Chem.* **281,** 34630–34639
50. Michel, S. L., and Berg, J. M. (2002) *Chem. Biol.* **9,** 667–668
51. Sharpe, B. K., Matthews, J. M., Kwan, A. H., Newton, A., Gell, D. A., Crossley, M., and Mackay, J. P. (2002) *Structure* **10,** 639–648
52. Garcia, G. A., and Goodenough-Lashhua, D. M. (1998) in *Modification and Editing of RNA* (Grosjean, H., and Benne, R., eds) pp. 135–168, American Society for Microbiology, Washington, D. C.
53. Cortese, R., Kammen, H. O., Spengler, S. J., and Ames, B. N. (1974) *J. Biol. Chem.* **249,** 1103–1108
54. Arena, F., Ciliberto, G., Ciampi, S., and Cortese, R. (1978) *Nucleic Acids Res.* **5,** 4523–4536
55. Hur, S., and Stroud, R. M. (2007) *Mol. Cell* **26,** 189–203
56. Droogmans, L., Roovers, M., Bujnicki, J. M., Tricot, C., Hartsch, T., Stalon, V., and Grosjean, H. (2003) *Nucleic Acids Res.* **31,** 2148–2156
57. Barraud, P., Golinelli-Pimpaneau, B., Atmanene, C., Sanglier, S., Van Dorsselaer, A., Droogmans, L., Dardel, F., and Tisné, C. (2008) *J. Mol. Biol.* **377,** 535–550
58. Guelorget, A., Roovers, M., Guérineau, V., Barbey, C., Li, X., and Golinelli-Pimpaneau, B. (2010) *Nucleic Acids Res.* **38,** 6206–6218
59. Anderson, J., Phan, L., Cuesta, R., Carlson, B. A., Pak, M., Asano, K., Björk, G. R., Tamame, M., and Hinnebusch, A. G. (1998) *Genes Dev.* **12,** 3650–3662
60. Anderson, J., Phan, L., and Hinnebusch, A. G. (2000) *Proc. Natl. Acad. Sci. U.S.A.* **97,** 5173–5178